Numerical Simulation of Ship Sailing In Regular Head Waves Using CFD Method

Hong Quang Nguyen and Ngoc Kien Vu*
Thai Nguyen University of Technology, 666, 3/2 Street, Tich Luong Ward,
Thai Nguyen City 251750, Vietnam
Email: quang.nguyenhong@tnut.edu.vn; kienvn@tnut.edu.vn

***Abstract*— The paper presents the results of a numerical simulation of a vessel sailing in regular head waves using CFD. The CFD study was carried out using the Unsteady RANSE method. The ship was sailing at serve speed in difference wave conditions. The pitch and heave motions of the ship and the ship resistance in different wave conditions been calculated. The results show that the ship resistance and ship motions depend strongly on the wavelength. The computation shows very integral quantities. Moreover, a comparison between EFD and CFD indicates that the predicted pitch and heave motions and the resistance are in fair agreement with the experimental data. The case study used to verify and validate the well-known benchmark KCS container ship.**

***Index Terms*— ship resistance, CFD, RANSE, Regular waves, motions.**

I. Introduction

Ordinarily, the sea-going vessel mainly operates in open waters but rarely do in calm weather. For this reason, the vessel is always affected by sea waves, and the ship resistance depends on different conditions. One of those is the sea state in that area, determined by wave height and period. The other factors are wave heading and ship characteristics. Accurate prediction of the added ship resistance on the wave is one of the key factors for the ship propulsion system's correct design.

The ship's problem added resistance and motion in wave condition have been extensively studied through experiments and numerical simulations employing CFD approaches. Among CFD methods used to solve ship hydrodynamics problems in general and added ship resistance in particular, the most popular process is the Reynold Averaged Navier-Stokes equation (RANSE) method, as it provides sufficient high accuracy for engineering purposes at the reasonable computational time [1], [2], [3]. Thus, this paper uses the RANSE method for predicting added ship resistance on waves. The Examples using RANSE CFD method to predict added ship resistance can be found in [4], [5], [6], [7], [8], [9]. The added ship resistance's magnitude depends on ship speed. As the increase of the ship speed, it increases and then decreases for the high speeds [9], [10] and [11] showed that in head waves, the added ship resistance is usually more significant than that in beam waves. Claus D. et al. presents heave and pitch results for ships sailing in head waves. The current study investigates the added ship resistance in short and long regular head waves using RANSE method. The flow in this work is calculated using RANSE solver Star-CCM+ and the motions of the ship are solved for pitch and heave by a 6 DOF, which is implemented in the RANSE code.

Manuscript received October 8, 2020; revised March 1, 2021.

II. Material And Method

A. Reynolds-Averaged Navier-Stokes Equations

The averaged continuity and momentum equations for incompressible flow without body forces, be written in tensor notation and Cartesian coordinates as [12]:

$$\frac{\partial(\rho\bar{u}_i)}{\partial x_i} = 0 \tag{1}$$

$$\frac{\partial(\rho\bar{u}_i)}{\partial t} + \frac{\partial}{\partial x_j}\left(\rho\bar{u}_i\bar{u}_j + \rho\overline{u_i'u_j'}\right) = -\frac{\partial\bar{p}}{\partial x_i} + \frac{\partial\bar{\tau}_{ij}}{\partial x_j} \tag{2}$$

Where ρ presents the fluid density, and are the averaged Cartesian components of the position and velocity vector, t represents the time, represents the Reynolds stress tensor, and represent the mean pressure and viscous stress tensor defined by:

$$\bar{\tau}_{ij} = \mu\left(\frac{\partial\bar{u}_i}{\partial x_j} + \frac{\partial\bar{u}_j}{\partial x_i}\right) \tag{3}$$

Where μ represents the dynamic viscosity.

A turbulence model should be applied to close Equations (1) and (2).

B. Turbulence Model

The turbulence model applied in the calculations was SST K-ω two equation-model because it solves two more the eddy viscosity equations. These are the turbulence kinetic energy (k), and turbulence dissipation rate ω equations.

SST K-ω solves transport equations for the turbulent kinetic energy *k* and the specific turbulence dissipation rate ω to evaluate the turbulent eddy viscosity μ_t that is described with following equation:

$$\mu_t = \rho kT \tag{4}$$

Where ρ is the fluid density, T is the turbulent time scale.

doi: 10.18178/ijmerr.10.4.183-188

The turbulent time scale (T) is calculated by Eqn. (5):

$$T = \min\left(\frac{a^*}{\omega}, \frac{a_1}{SF_2}\right) \tag{5}$$

Where a*, a_1 are model coefficients, F_2 is a blending function, S is defined by Equation (6).

$$S = \left|\bar{S}\right| = \sqrt{2\bar{S} : \bar{S}^T} = \sqrt{2\bar{S} : \bar{S}} \tag{6}$$

The mean strain rate tensor $\bar{S}$ S is define by:

$$\bar{S} = \frac{1}{2}(\nabla\bar{v} + \nabla\bar{v}^T) \tag{7}$$

Where $\bar{v}$ is the mean velocity.

The blending function F_2 are calculated as:

$$F_2 = \tanh\left(\left(\max\left(\frac{2\sqrt{k}}{\beta^*\omega d'}, \frac{500v}{d^2\omega}\right)\right)^2\right) \tag{8}$$

Where: β^* is a model coefficient, d is the distance to the wall.

The transport equations for k and ω are defined as follows:

$$\frac{\partial}{\partial t}(\rho k) + \nabla\cdot(\rho k\bar{v}) = \nabla\cdot\left[(\mu + \sigma_k\mu_t)\nabla k\right] + \\ + P_k - \rho\beta^* f_{\beta^*}(k\omega - k_0\omega_0) + S_k \tag{9}$$

$$\frac{\partial}{\partial t}(\rho\omega) + \nabla\cdot(\rho\omega\bar{v}) = \nabla\cdot\left[(\mu + \sigma_\omega\mu_t)\nabla\omega\right] + \\ + P_\omega - \rho\beta f_\beta(\omega^2 - \omega_0^2) + S_\omega \tag{10}$$

Where: σ_k and $\sigma_\omega, C_{\varepsilon 1}$ and $C_{\varepsilon 2}$ are model coefficients, P_k and P_ω are production terms, μ is the dynamic viscosity, f_{β^*}, f_β are the free-shear and vortex-stretching modification factors, respectively, k_0 and ω_0 are the ambient turbulence values, S_ω and S_k are user-specified source terms.

Production terms P_k and P_ω are given by Eqn. (8) and Eqn. (9), respectively:

$$P_k = G_k + G_{nl} + G_b;\ \ P_\omega = G_\omega + D_\omega \tag{11}$$

$$P_k = G_k + G_b;\ P_\omega = G_\omega \tag{12}$$

Where D_ω and G_ω are Cross-diffusion term and specific dissipation production respectively, those are defined as follows:

$$G_\omega = \rho\gamma\left[\left(S^2 - \frac{2}{3}(\nabla\cdot\bar{v})^2\right) - \frac{2}{3}\omega\nabla\cdot\bar{v}\right] \tag{13}$$

$$D_\omega = 2\rho(1-F_1)\sigma_\omega\frac{1}{\omega}\nabla k\cdot\nabla\omega \tag{14}$$

The blending function F_1 combines the near-wall contribution of a coefficient with its value far away from the wall and is defined as:

$$F_1 = \tanh\left(\left[\min\left(\max\left(\frac{\sqrt{k}}{0.09\omega d}, \frac{500v}{d^2\omega}\right), \frac{2k}{d^2 CD_{k\omega}}\right)\right]^4\right) \tag{15}$$

Where: d is the distance to the wall, v is the kinematic viscosity, $CD_{k\omega}$ is the cross-diffusion coefficient is given by Equation 16.

$$CD_{k\omega} = \max\left(\frac{1}{\omega}\nabla k\cdot\nabla\omega, 10^{-20}\right) \tag{16}$$

III. Numerical Simulations

A. Reference Vessel and Wave Conditions

The container ship KCS with appended in model scale (see Fig. 1 and Table I) is used as a reference vessel in this study. The ship is considered at the Froude number of 0.26, which corresponds to a service speed of 1.701 m/s and the Reynolds number Re=6.517.106.

The wave conditions are listed in Table II, corresponding to the towing tank [4]. The regular waves are generated employing the Stokes wave theory. The simulation wavelength range is from 3.950m to 11.851m, corresponding to the shortest wave condition (W1) and the most extended wave condition (W5).

TABLE I. Parameters of the KCS Model Test Case

Description		Ship [13]	Model
Scale factor	λ	-	37.89
Length between perpendiculars	L_{PP} [m]	230.00	6.07
Breadth of ship	B [m]	32.20	0.85
Draft of ship	T [m]	10.78	0.285
Wetted surface	S_W [m2]	9530	4.12
Volume	∇ [m3]	52186	0.9571
Ship speed	V [m/s]	12.415	2.017

Figure 1. KCS container ship geometry

TABLE II. WAVE CONDITIONS ARE CONSIDERED IN SIMULATION

Case study		W1	W2	W3	W4	W5
Wave length	λ_W [m]	3.950	5.165	6.980	8.320	11.851
Wave height	H [m]	0.063	0.079	0.125	0.150	0.186
Wave steepness ratio	$k\zeta$ [-]	0.052	0.054	0.056	0.056	0.055
Ratio between Wave length and ship length	$\lambda_W \backslash L_{PP}$	0.650	0.850	1.150	1.370	1.950

B. Computational Procedure

To determine the wave added ship resistance, R_{AW}. The procedure includes three key steps. In the first step, the ship resistance in calm water, R_T, corresponding to specific ship speed, is determined. In the second one, the mean ship resistance in waves, R_{WAVE}, is computed. The ship is capable to pitch and heave freely. However, its other rest degrees of freedom were suppressed. Finally, the wave added ship resistance can be computed by eliminating ship resistance in the calm water from the time-averaged longitudinal force in waves. In the same manner, the frictional part of added ship resistance is determined. Regarding this procedure, applying the same numerical grids and test setups for all computation cases can minimize possible errors due to spatial and temporal discretization, model test scale impacts, and iterative computational techniques.

The calm water ship resistance coefficient, C_T is defined as follows:

$$C_T = \frac{R_T}{0.5\rho V^2 S_W} \tag{17}$$

R_T represents calm water ship resistance, V represents ship speed, ρ represents water density, and S_W represents wetted hull ship.

Due to model tests are unsuitable for predicting the frictional ship resistance component, the ship frictional resistance coefficient is mainly defined, relying on the ITTC 78 guidelines [14] as follows:

$$C_F = \frac{0.075}{(\log_{10} \mathrm{Re} - 2)^2} \tag{18}$$

Where *Re* represents the Reynolds number, $\mathrm{Re} = VL_{PP}/\upsilon$, L_{PP} is the length between perpendiculars of the ship, and υ is kinematic viscosity of water. Then, the frictional resistance, R_F, can be calculated as the following equation:

$$R_F = \frac{1}{2} C_F \rho V^2 S_W \tag{19}$$

The added wave ship resistance caused by waves (ΔR_{wave}) is estimated by Eq. (20):

$$\Delta R_{WAVE} = R_{WAVE} - R_T \tag{20}$$

Response amplitude operators are plotted against the dimensionless wave frequency $\bar{\omega}$ is determined as follows:

$$\bar{\omega} = \sqrt{L/\lambda_W} \tag{21}$$

C. Numerical Setup

For ship resistance in calm water simulation in general and ship resistance in head waves in particular, the ship hull is symmetric, so to save computational resource and complexity, only port side (the starboard side) of the ship hull is simulated. The size of the computational domain was orientated to the length of the ship models. According to the recommendations of ITTC [15], the upstream boundary is located at 1.5Lpp from FP, the downstream boundary is located at 2.5Lpp after aft of AP. The lateral boundary is located at 2.5Lpp away from the midship plane. The bottom and top boundaries are located at 2.5Lpp and 1.25Lpp away from the free surface, respectively. Artificial wave damping was employed to eliminate the unwanted effect of the reflected waves from the side and outlet.

The boundary conditions were selected on the domain boundaries. The ship hull as follows: a constant velocity condition was used on the inlet, bottom, and top; No-slip wall condition on the ship hull; the hydrostatic pressure was specified at outflow; symmetry condition at symmetry plane and sidewall. The free surface is located at z = 0. The ship stern (aft perpendicular) is located at x = 0. The average Y+ value on the submerged part of the hull was 40. Therefore, the wall function is applied to the wall treatment to reduce the mesh size.

The grid used in this study was a trimmed grid. The mesh generation process is driven by specifying base mesh size, relative to which all spacing is defined. The grids were refined around the hull region near the free surface, ship stern and bow, and rudder. The grid near the free surface was refined to capture the elevation of the waves precisely. To obtain the correct flow behaviour near the walls of wetted surface, prism layers were employed.

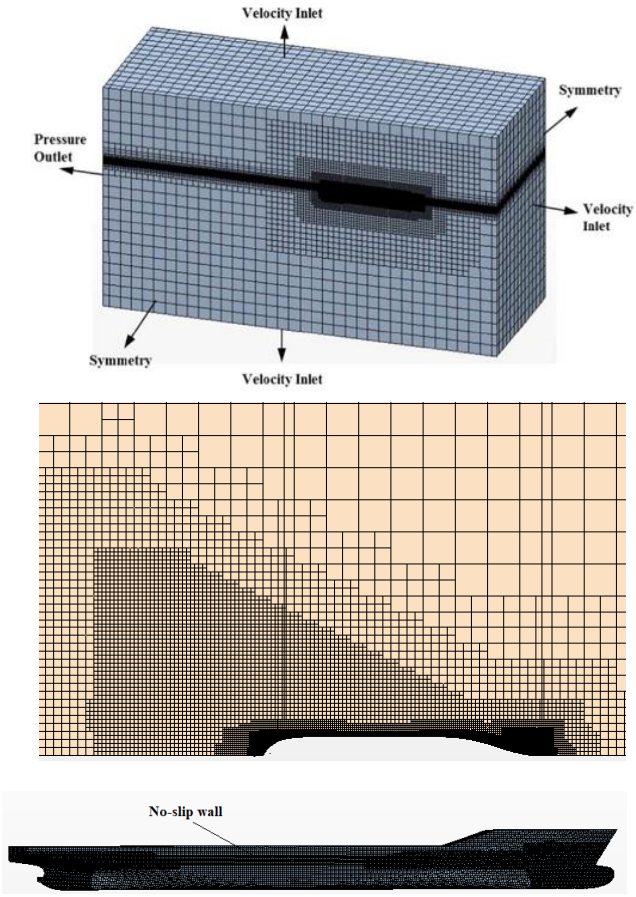

Figure 2. Mesh and boundary condition

An unsteady RANSE method was used to predict the ship motions and ship resistance in regular head waves utilizing commercial solver Star-CCM+. The volume of fluid method (VOF) and the finite volume method (FVM) were used for the free surface capturing and spatial discretization, respectively. Employing a predictor-corrector method could help to solve the flow equations. Convection and diffusion components in the RANSE equations were discretized by a second-order upwind scheme and a central difference scheme. The turbulence model applied in the calculations was SST K-ω two equation-model. It solves two additional eddy viscosity equations: the turbulence kinetic energy (k), and turbulence dissipation rate (ε or ω) equation. This model indicates to be capable of predicting ship hydrodynamics accurately. Another reason is that these are the most applied by CFD researchers (80 percent of the Gothenburg 2010 Workshop submissions used k- ω two equation-model) [16]. DFBI - Dynamic Fluid Body Interaction is employed to consider ship motions in heave and pitch directions.

Regarding current simulation, at least 5 inner iterations are employed on each time step. The non-dimensional time step is set to Δt=0.005, which provides 85-time steps per encounter period.

IV. Results and Discussion

A. Verification and Validation Study

One of the key issues determining the numerical level of accuracy is grid size. Thus, first of all, it is necessary to execute an extensive verification for grid size. The mesh sensitivity analysis is implemented for the calm water condition (W0) to separate the skin friction prediction from the waves' influence. Verification study for mesh sensitivity is performed with three grids, so that coarse (grid#3), medium (grid#2) and fine grid (grid#1) with the refinement ration r_i equal to $\sqrt{2}$ (According to the ITTC procedure [17]) that are corresponding to the cells number of 1.35, 3.72 and 9.75 million, respectively. The convergence ratio is determined as follows:

$$R_G = \frac{\varepsilon_{21}}{\varepsilon_{32}} \tag{22}$$

Where $\varepsilon_{21}= S_2 - S_1$ and $\varepsilon_{32}= S_3 - S_2$ are the difference between solution achieved using medium mesh (S_2) and fine mesh (S_1) and the difference between solution achieved using coarse (S_3) and medium (S_2) input parameter.

There are three kinds of possible convergence conditions: divergence ($R_G > 1$), oscillatory convergence ($R_G < 0$), and monotonic convergence ($0 < R_G < 1$).

The results of the sensitivity study for the calm water condition simulation is illustrated in Table III. It can be observed from Table III that monotonic convergence was achieved, and predicted total resistance in calm water agrees well with the experimental data with a deviation is less than 2.0% (for medium mesh). Therefore, the medium mesh was used in further studies.

TABLE III. Ship Resistance in Calm Water Condition for Diffirent Mesh Sizes

Parameter		EFD [4]	V&V study			ε_{21}	ε_{32}	R_G
			Grid #3	Grid #2	Grid #1			
$C_T.10^3$	Value	3.835	3.702	3.759	3.805	-0.046	-0.057	0.81
	E%D	/	3.47	1.98	0.78	/	/	/
$C_F.10^3$	Value	/	2.928	2.953	2.975	-0.022	-0.025	0.88
	E%D	/	/	/	/	/	/	/
$C_P.10^3$	Value	/	0.774	0.806	0.83	-0.024	-0.032	0.75
	E%D	/	/	/	/	/	/	/

B. Resistance and Ship Motions in Waves

Five head-wave simulations carry out the resistance due to waves changing the wave height and length. The ship motion and resistance in wave analysis are performed by applying a Fourier series reconstruction to extract the resultant signals' primary harmonics. Table IV illustrates a summary of the mean calculated resistance and experimental mean value results. This consists of the mean total resistance coefficient on wave C_{WAVE}, mean pitch angle θ , and mean heave z normalized by wave amplitude ζ and steepness ratio $k\zeta$, respectively.

TABLE IV. MEAN RESULTS FOR THE SHIP RESISTANCE AND SHIP MOTIONS IN REGULAR HEAD WAVES

C_{WAVE}	W1	W2	W3	W4	W5
CFD	7.036	8.114	13.687	13.545	10.285
EFD	7.243	8.254	13.167	12.985	9.852
E%D [%]	2.86	1.70	-3.95	-4.31	-4.40
z/ζ					
CFD	-0.753	-0.569	-0.255	-0.221	-0.197
EFD	-0.819	-0.618	-0.268	-0.239	-0.211
E%D [%]	8.06	7.93	4.85	7.53	6.64
$\theta/k\,\zeta$					
CFD	-0.1173	-0.1424	-0.0024	-0.0063	-0.0598
EFD	-0.1081	-0.1313	-0.0025	-0.0067	-0.0572
E%D [%]	-8.51	-8.45	4.00	5.97	-4.55

It can be observed from Table IV that the predicted mean ship resistance coefficient in wave agrees well with the experimental value in all cases. In case of W5, the maximum wavelength deviation is 4.40%. The relative errors of the mean pitch and heave motions of the ship are more significant than the resistance errors. Their absolute value is significantly smaller than ship resistance. The mean heave motion of the ship is evaluated to within 8.00% of the experimental value where the most considerable error for case W1 is equal to 8.06%. The most massive difference in the mean pitch motion of the ship is found in case W2.

The wave elevation contour for the calm-water condition and five waves' conditions are shown in Fig. 3.

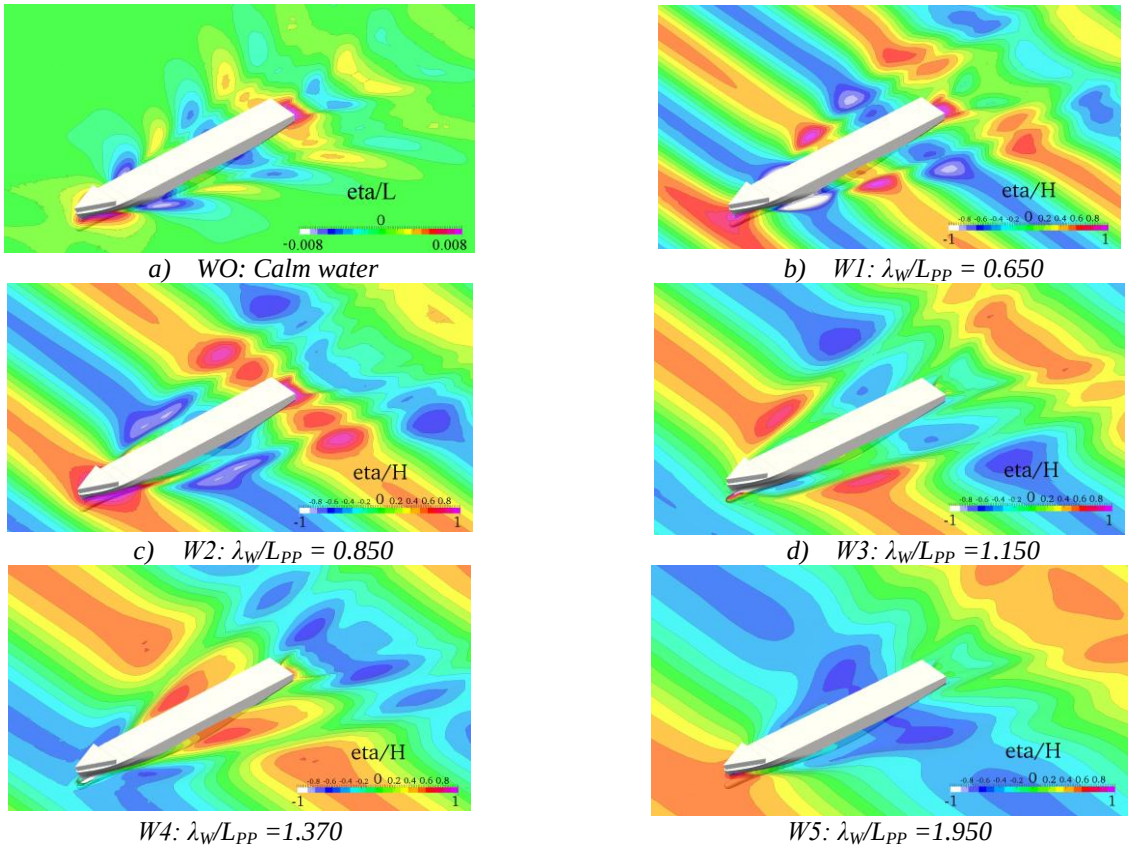

a) WO: Calm water

b) W1: λ_W/L_{PP} = 0.650

c) W2: λ_W/L_{PP} = 0.850

d) W3: λ_W/L_{PP} =1.150

W4: λ_W/L_{PP} =1.370

W5: λ_W/L_{PP} =1.950

Figure 3. Wave elevation contour plot

V. Conclusion

In the current research, the three-dimensional incompressible viscous Unsteady RANSE CFD approach has been used to investigate the ship motions and resistance in wave conditions. Six case studies at the different wavelengths are performed to assess the influence of wave parameters on ship motions and resistance. Therefore, the following conclusions can be made:

-The evaluation of the ship resistance and motions in wave agrees well with the experimental value over an extensive range of wave conditions.

-The solver is applied to define the most affected design waves resulting in an extreme heave motion of the ship.

-Generally, the ship resistance and ship motions in wave conditions depend on wavelength. The impact level of wavelength on ship resistance depends on steepness ratio, ship's hull form, ship's draft, and speed.

Conflict of Interest

The authors declare that the submitted work has no conflict of interest

Acknowledgment

This research was funded by the Thai Nguyen University of Technology, No. 666, 3/2 street, Thai Nguyen City, Viet Nam.

References

[1] T. N. Tu, et al., "Numerical study on the influence of trim on ship resistance in trim optimization process," *Naval Engineers Journal*, vol. 130, no. 4, pp. 133-142, 2018.

[2] V. C. Huynh, G. T. T., "Improving the accuracy of ship resistance prediction using computational fluid dynamics tool," *International Journal on Advanced Science, Engineering and Information Technology*, vol. 10, no. 1, 2020.

[3] M. I. Ghazali, Z. H., W. A W. Ghopa, A. A. Abbas, "Computational fluid dynamic simulation on NACA 0026 airfoil with V-groove riblets," *International Journal on Advanced Science, Engineering and Information Technology*, vol 6, no. 4.

[4] C. D. Simonsen, et al., "EFD and CFD for KCS heaving and pitching in regular head waves," *Journal of Marine Science and Technology*, vol. 18, no. 4, pp. 435-459, 2013.

[5] S. Sigmund and O. J. O. E. El Moctar, "Numerical and experimental investigation of added resistance of different ship types in short and long waves," *Ocean Engineering*, vol. 147, pp. 51-67, 2018.

[6] H. Sadat-Hosseini, et al., "CFD verification and validation of added resistance and motions of KVLCC2 with fixed and free surge in short and long head waves," *Ocean Engineering*, vol. 59, pp. 240-273, 2013.

[7] H. Söding and V. J. S. T. R. Shigunov, "Added resistance of ships in waves," *Ship Technology Research*, vol. 62, no. 1, pp. 2-13, 2015.

[8] M. Kim, et al., "Estimation of added resistance and ship speed loss in a seaway," *Ocean Engineering*, vol. 141, pp. 465-476, 2017.

[9] H. Zeraatgar and F. J. J. O. M. E. Abed Hossein Nezhad, "Added resistance & drift force analysis in regular and irregular waves," *Ocean Engineering*, vol. 2, no. 1, pp. 70-85, 2006.

[10] M. P. A. Ghani and J. J. J. J. J. M. Julait, "Prediction of added resistance of ship due to regular head waves," *Journal of Marine Engineering*, vol. 26, no. 2, 2008.

[11] H. Zeraatgar and F. J. J. O. M. E. Abed Hossein Nezhad, "Added resistance & drift force analysis in regular and irregular waves," *Journal of Marine Engineering*, vol. 2, no. 1, pp. 70-85, 2006.

[12] J. H. Ferziger, M. Perić, and R. L. Street, "Computational methods for fluid dynamics," vol. 3. 2002, Springer.

[13] Simman. [Online]. Available: http://www.simman2008.dk/KCS/kcs_geometry.htm.

[14] The 1978 ITTC Performance Prediction Method for Single Screw Ships. [Online]. Available: https://ittc.info/media/2037/75-02-03-014.pdf.

[15] ITTC, (2014). Recommended procedures and guidelines 7.5-03-02-04. [Online]. Available: https://ittc.info/media/4198/75-03-02-04.pdf.

[16] Z. Yong, et al., "Turbulence model investigations on the boundary layer flow with adverse pressure gradients," vol. 14, no. 2, pp. 170-174, 2015.

[17] ITTC Specialist Committee. (2017). Recommended procedures and guidelines - uncertainty analysis in CFD verification and validation methodology and procedures. [Online]. Available: https://www.ittc.info/media/8153/75-03-01-01.pdf.

Hong Quang Nguyen received the Master's degree in control engineering and automation from Hanoi University of Science and Technology (HUST), Viet Nam, 2012 and a Ph.D. from Thai Nguyen University of Technology (TNUT), Vietnam, 2019. He is currently a lecturer at the Faculty of Mechanical, Electrical, and Electronic Technology, Thai Nguyen University of Technology (TNUT). His research interests include electrical drive systems, control systems and its applications, adaptive dynamic programming control, robust nonlinear model predictive control, motion control, and mechatronics.

Ngoc Kien Vu was born in 1983. He received Master's degree in Automatic Control in 2011; Ph.D. in Automatic Control in 2015 from Thai Nguyen university of technology. From 2006 to now, he was a lecturer at Thai Nguyen University of technology.
His main researches are model order reduced algorithm, automatic.